Singularities of meniscus at the V-shaped edge

Mars M. Alimov[1] and Konstantin G. Kornev[2]

[1] Kazan Federal University, Kazan, Russia

[2]Department of Materials Science & Engineering, Clemson University, Clemson, SC

Abstract

An understanding of the capillary rise of the meniscus formed on the V-shaped fibers is crucial for many applications. We classified the cases when the meniscus cannot be smooth by analyzing the local behavior of the solutions to the Laplace equation of capillarity near the sharp edge. The V-angle and two contact angles that the meniscus forms on two chemically different sides of the fiber form a 3D phase space. Smooth menisci constitute a special domain in this 3D space. The constructed diagram allows one to separate the solutions with smooth and non-smooth menisci. The obtained criteria were illustrated using chemically inhomogeneous plates, blades, square corners, and Janus V-shaped edges.

In the Jurin capillary rise experiment, a fiber is immersed perpendicularly to the free liquid surface [1]. The air/liquid interface deforms into a meniscus. Depending on the fiber wettability, the contact line, separating wet and dry parts of the fiber surface, can bend into different configurations. The shapes of the contact line and meniscus are very sensitive to the surface properties of a fiber [2-6]. In many cases, classification of the substrate wettability is associated with the behavior of the contact line [6]. In design of omniphobic materials, one needs to understand the effect of the fiber shape on the formation of singularities on the contact line [7, 8]. When the fiber surface is not smooth and have some V-shaped grooves, Concus and Finn [9] showed that the nonlinear Laplace equation of capillarity may have a family of solutions with the infinite first derivative at the wetting boundary. It is therefore instructive to analyze the behavior of meniscus at the fiber surface having not only some V-shaped grooves, but also the V-shaped sharp edges. An asymptotic solution of the Laplace equation of capillarity near the sharp V-type edges revealed the criteria for the development of non-smooth menisci.

In the Cartesian system of coordinates (x, y, z), the meniscus profile $z = h(x, y)$ describes the liquid elevation above the reference plane (x, y), which coincides with the horizontal liquid level far away from the fiber. The center of coordinates is chosen at the V-edge O shown in Fig. 1. The Laplace law of capillarity [10], $\sigma(1/R_1 + 1/R_2) - \rho g H = 0$ is employed to describe the meniscus shape where the first term in this equation is the mean curvature defined by two principle radii of curvatures R_1 and R_2; the second term is the hydrostatic pressure, σ is the surface tension

of the liquid, ρ is its density, and g is acceleration due to gravity. The Young-Laplace equation is used to formulate the boundary condition at the surfaces of each face of the wedge with different contact angles, γ^+ and γ^- [6, 10, 11]. It is convenient to rewrite the mean curvature in terms of the outward normal vector $\mathbf{N}$ to the meniscus surface, $(1/R_1 + 1/R_2) = -\nabla\cdot\mathbf{N}$, where this vector is expressed through the surface elevation as $\mathbf{N} = \left(1+|\nabla h|^2\right)^{-1/2}\left(-\partial h/\partial x, -\partial h/\partial y, 1\right)$ [12]. Thus, the mathematical model is written as [13, 14]

$$\Omega: \qquad \nabla\cdot\left[\left(1+|\nabla h|^2\right)^{-1/2}\nabla h\right] - \rho g h/\sigma = 0, \tag{1.1}$$

$$\Gamma^{\pm}: \qquad \left(1+|\nabla h|^2\right)^{-1/2}\frac{\partial h}{\partial n} = -\cos\gamma^{\pm}. \tag{1.2}$$

where Ω is the domain occupied by the liquid, and $\mathbf{n}$ is the outward unit normal vector to the boundaries $\Gamma^{\pm}$, Fig. 1*a*).

Since we are interested only in the behavior of meniscus in the vicinity of the sharp edge, the boundary condition at infinity is relaxed. First we need to define what we mean under the smooth and singular menisci. Writing eq. (1.1) in the form $-\nabla\cdot\mathbf{N} = \rho g h/\sigma$ one immediately infers that the normal vector $\mathbf{N}$ must be continuous and differentiable in Ω, hence the meniscus should be smooth in Ω. Singularities are permissible only at the boundary $\Gamma = \Gamma^+ \cup \Gamma^-$. These singularities can be generated, for example, by the singularities of the boundary.

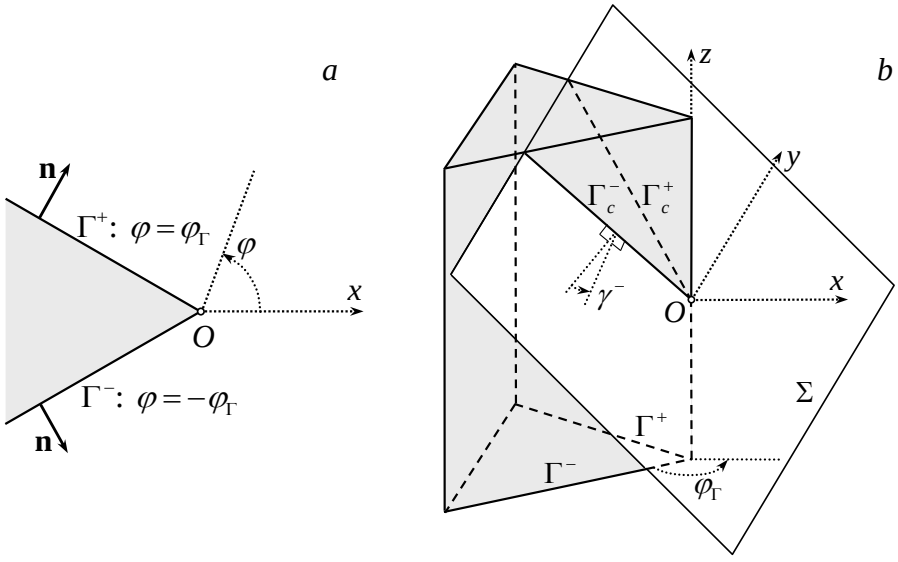

Figure 1. (*a*) Cross-section of the corner modeling a sharp edge-like singularity at the fiber surface; (*b*) A schematic of meniscus surface Σ meeting the wedge at the contact angles γ^- (wetting case). This locally flat surface of the meniscus can exist only within a certain window of the physical parameters specified by inequality $\Phi > 0$, where Φ is defined by eq. (1.12).

Consider for a moment the general case of a complex-shaped fiber. To accommodate the effect of the fiber shape in the definition of the smooth meniscus, we will call the meniscus smooth when its normal vector $\mathbf{N}$ changes continuously along the contact line $\Gamma_c = \Gamma_c^+ \cup \Gamma_c^-$ and the contact line is described by a continuous function $h(x,y)$, $(x,y) \in \Gamma^{\pm}$. This condition is sufficiently weak because it permits one of the components of the gradient vector $\nabla h(x,y)$ to be singular. For example, meniscus on a completely wettable circular cylinder, $\gamma = 0$, is smooth. At the same time, the radial derivative of the function is infinite at the fiber surface due to the boundary condition, $\partial h / \partial r|_{\Gamma} \to \infty$. Following the change of the normal vector $\mathbf{N}$ along the contact line Γ_c: $h|_{\Gamma} = h_{\Gamma} = const$, one observes that it changes continuously: the angular derivative of the h-function is zero $\partial h / \partial \varphi|_{\Gamma} = 0$.

If at some point of the surface both components of the gradient vector $\nabla h(x,y)$ tend to infinity, one cannot define the normal vector $\mathbf{N}$ at this point. Hence this point will be singular. For example, the contact line may form a cusp at the fiber surface at this point.

The goal of this Letter is to find the criteria for the meniscus smoothness near the V-shaped edge. To analyze the behavior of meniscus near the edge, we introduce the cylindrical system of coordinates (r,φ) measuring angle φ with respect to the x-axis, and distance r with respect to the vertex O in Fig. 1*a*). We assume that the edge is symmetric with respect to the axis $\varphi = 0$. However, since the edge is chemically inhomogeneous, the meniscus profile $h(r,\varphi)$ is not symmetric with respect to the axis $\varphi = 0$, forming two different contact angles $\gamma^{\pm}$ on different sides of the edge.

Rewriting eq. (1.1) and boundary condition (1.2) in the cylindrical system of coordinates, and imposing the symmetry condition at the line $\varphi = 0$, one formulates the boundary value problem (1.1) – (1.2) as

$$\frac{1}{r}\frac{\partial}{\partial r}\left(Gr\frac{\partial h}{\partial r}\right) + \frac{1}{r}\frac{\partial}{\partial \varphi}\left(\frac{G}{r}\frac{\partial h}{\partial \varphi}\right) - \frac{\rho g}{\sigma}h = 0, \tag{1.3}$$

$$G\frac{\partial h}{\partial \varphi}\bigg|_{\varphi = \pm\varphi_{\Gamma}} = \pm r\cos\gamma^{\pm}, \tag{1.4}$$

where

$$G = (1+|\nabla h|^2)^{-1/2} = \left[1 + \left(\frac{\partial h}{\partial r}\right)^2 + \frac{1}{r^2}\left(\frac{\partial h}{\partial \varphi}\right)^2\right]^{-1/2}. \tag{1.5}$$

The analysis of the meniscus smoothness is reduced to the analysis of coefficients of the Taylor series with respect to the r-component. The following Taylor series represents the solution $h(r,\varphi)$ as $r \to 0$:

$$r \ll 1: \qquad h(r,\varphi) = F^o + \sum_{k=1}^{\infty} r^k F_k(\varphi). \tag{1.6}$$

where F^o – is a constant. The terms of the form $h(r,\varphi) \approx r^\alpha F_\alpha(\varphi)$, with $\alpha < 1$, and $h(r,\varphi) \approx F_0(\varphi)$, with $F_0'(\varphi) \neq 0$, and other terms containing singularities (for example, logarithmic and the like) are not considered because they would lead to a non-smooth meniscus in the vicinity of point O.

Substituting the asymptotic series (1.6) into system of equations (1.3) – (1.5) and collecting the terms of the same r^k order, we obtain a set of the boundary value problems for each function $F_k(\varphi)$. The terms of the order $O(r)$ provide the next set of equations for $F_1(\varphi)$:

$$\frac{F_1 + F_1''}{\left[1 + F_1^2 + (F_1')^2\right]^{1/2}} - \frac{F_1 (F_1')^2 + F_1'' (F_1')^2}{\left[1 + F_1^2 + (F_1')^2\right]^{3/2}} = 0, \tag{1.7}$$

$$\left. \frac{F_1'}{\left[1 + F_1^2 + (F_1')^2\right]^{1/2}} \right|_{\varphi = \pm\varphi_\Gamma} = \pm \cos\gamma^{\pm}. \tag{1.8}$$

Equation (1.7) can be factorized as

$$(F_1 + F_1'')(1 + F_1^2)\left(1 + F_1^2 + F_1'^2\right)^{-3/2} = 0.$$

Therefore, the general solution of this equation is

$$F_1(\varphi) = A_1 \cos\varphi + A_2 \sin\varphi, \tag{1.9}$$

where constants A_1 and A_2 have to be determined. Substituting this general solution (1.9) into eq. (1.8), one obtains

$$\frac{\mp A_1 \sin\varphi_\Gamma + A_2 \cos\varphi_\Gamma}{\sqrt{1 + A_1^2 + A_2^2}} = \pm \cos\gamma^{\pm},$$

or $$A_1 = -\frac{\cos\gamma^+ + \cos\gamma^-}{2\sin\varphi_\Gamma}\sqrt{1 + A_1^2 + A_2^2}, \qquad A_2 = \frac{\cos\gamma^- - \cos\gamma^+}{2\cos\varphi_\Gamma}\sqrt{1 + A_1^2 + A_2^2}. \tag{1.10}$$

These two equations have to be solved for A_1 and A_2. The square root $\sqrt{1 + A_1^2 + A_2^2}$ is understood as strictly positive. Squaring both sides of eqs. (1.10) and solving the resulting equations for A_1^2 and A_2^2, one obtains

$$A_1^2 = \frac{1}{\Phi}(\cos\gamma^+ + \cos\gamma^-)^2 \cos^2\varphi_\Gamma, \qquad A_2^2 = \frac{1}{\Phi}(\cos\gamma^+ - \cos\gamma^-)^2 \sin^2\varphi_\Gamma, \tag{1.11}$$

where

$$\Phi = (1-\cos^2\gamma^+-\cos^2\gamma^-) - 2\cos\gamma^+\cos\gamma^-\cos 2\varphi_\Gamma - \cos^2 2\varphi_\Gamma . \qquad (1.12)$$

Since the left hand sides of eqs. (1.11) must be strictly positive, we obtain a natural solvability condition as, $\Phi > 0$. This conditions imposes a constraint on the triple $\gamma^+, \gamma^-, \varphi_\Gamma$ narrowing the space of these parameters where smooth solution (1.6) exists. This smooth solution has the following asymptotic representation in the vicinity of point O:

$$r \ll 1: \qquad h(r,\varphi) \approx F^o + A_1 r\cos\varphi + A_2 r\sin\varphi \qquad \Leftrightarrow \qquad h(x,y) \approx F^o + A_1 x + A_2 y . \qquad (1.13)$$

The last form (1.13) explicitly shows that the meniscus approaches the edge as a planar surface.

Before analyzing the 3D phase diagram of wetting for the triple $\gamma^+, \gamma^-, \varphi_\Gamma$, it is instructive to illustrate the richness of possibilities of wetting transitions by considering some particular geometries and chemical inhomogeneities allowing to reduce the 3D phase diagram to a 2D case.

Chemically inhomogeneous plate. Consider a meniscus formed on a plate $x = 0$, when two parts of the plate are chemically different. In our notations, this example corresponds to the case when $\varphi_\Gamma = \pi/2$; $\gamma^+, \gamma^- \in [0, \pi]$. We assume that the angle γ^+ corresponds to the semi-infinite plane $\{x = 0,\ y > 0\}$, while the angle γ^- corresponds to another semi-infinite plane $\{x = 0,\ y < 0\}$. In these notations, inequality $\Phi > 0$ takes on the form

$$(\cos\gamma^+ - \cos\gamma^-)^2 < 0 . \qquad (1.14)$$

This strong restriction on the contact angles does not permit solutions (1.13) to occur: meniscus cannot approach this separation line without formation of some singularity. However, eq. (1.14) cannot be directly applied to the limiting case $\gamma^+ = \gamma^- = \gamma$ which is singular for eqs. (1.11). Hence it requires a special care to analyze it. Turning to the original eqs. (1.10), we see that in the limiting case $\gamma^+ = \gamma^- = \gamma$, the constant $A_2 = 0$, i.e. it is always equal to zero. The constant A_1 is determined from equation $A_1 = -\cos\gamma\sqrt{1 + A_1^2}$, which has the unique solution $A_1 = -\cos\gamma / \sqrt{1-\cos^2\gamma}$. This implies that the model has no contradiction with the experiment and any planar substrate will form a smooth meniscus.

Another instructive example is a thin blade. We assume that the blade thickness is so small that one can model it as a mathematical cut along the line $\{y = 0,\ x < 0\}$.

Blade, $\varphi_\Gamma = \pi$; $\gamma^+, \gamma^- \in [0, \pi]$. The solvability condition $\Phi > 0$ takes on the form $(\cos\gamma^+ + \cos\gamma^-)^2 < 0$. This condition cannot be satisfied. Again, the case of a chemically uniform blade $\gamma^+ = \gamma^- = \pi/2$ is singular. However, there is one physically meaningful case when meniscus can approach the blade perpendicularly to its sides, $h \equiv 0$. In all other cases, only non-smooth menisci will be formed on the blade.

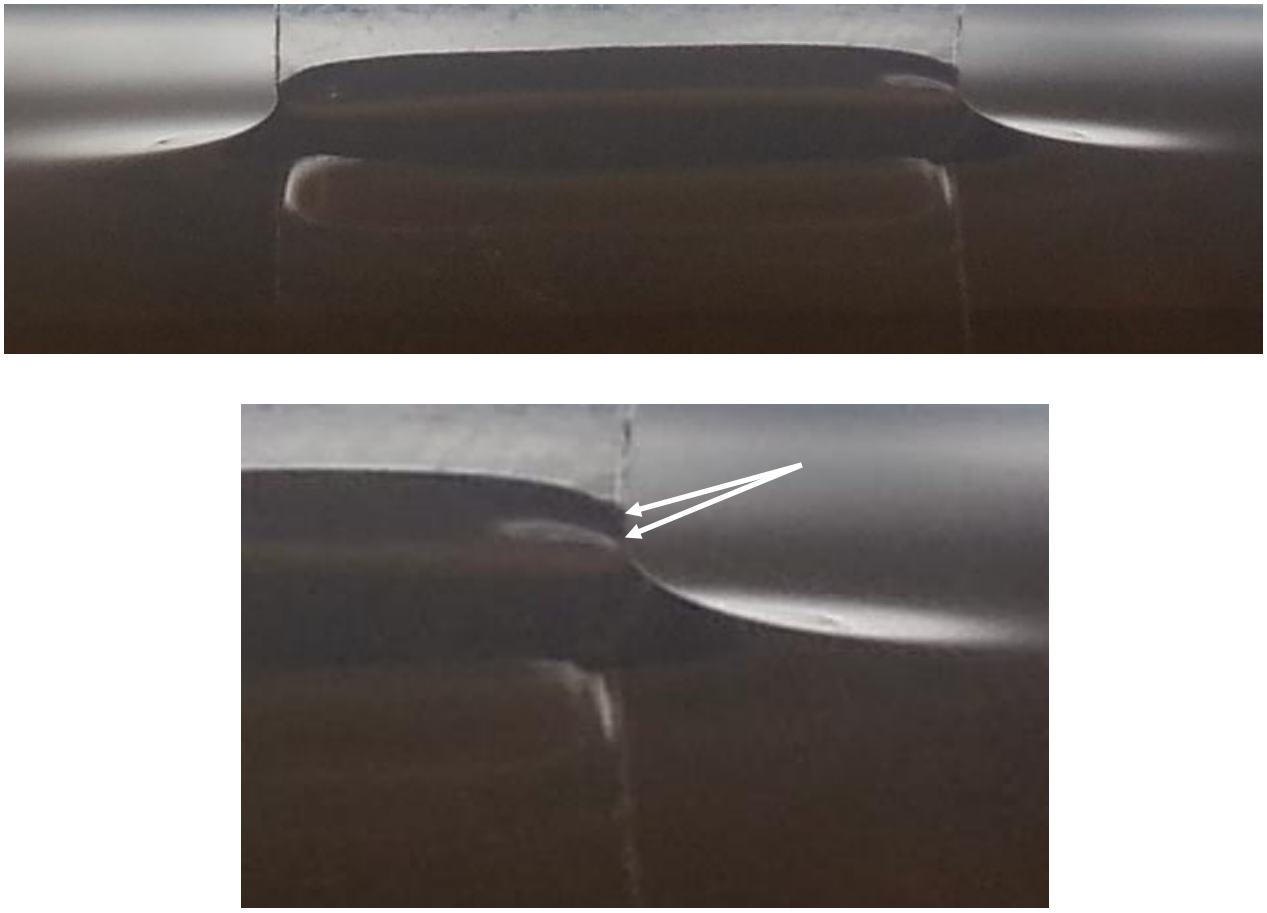

Figure 2. Illustration of the meniscus shape at the edge of a polypropylene film that has been dipped in a syrup. The arrows on the magnified image indicate a jump of the end point of the contact line along the film edge.

Consider non-trivial examples when the solvability condition $\Phi > 0$ can be analyzed analytically.

Interiors and exteriors of the square corners, $\varphi_\Gamma = \pi/4$ and $\varphi_\Gamma = 3\pi/4$; $\gamma^+, \gamma^- \in [0, \pi]$. In these two cases, the solvability condition $\Phi > 0$ is simplified to the following inequality

$$\cos^2\gamma^+ + \cos^2\gamma^- < 1 \qquad or \qquad \cos^2\gamma^+ < \sin^2\gamma^- . \tag{1.15}$$

In the plane (γ^+, γ^-), which can be called the phase diagram of wetting transitions, inequality (1.15) selects the interior of the domain with the boundary, which is specified by the following equations

$$\gamma^- = \arcsin|\cos\gamma^+| = \arcsin|\sin(\pi/2 - \gamma^+)| = \begin{cases} \pi/2 - \gamma^+, & where \ \ \gamma^+ \in [0, \pi/2]; \\ \gamma^+ - \pi/2, & where \ \ \gamma^+ \in [\pi/2, \pi]. \end{cases} \tag{1.16}$$

and

$$\gamma^{-} = \pi - \arcsin|\cos\gamma^{+}| = \pi - \arcsin|\sin(\pi/2 - \gamma^{+})| = \begin{cases} \pi/2 + \gamma^{+}, & where\ \ \gamma^{+} \in [0, \pi/2]; \\ 3\pi/2 - \gamma^{+}, & where\ \ \gamma^{+} \in [\pi/2, \pi]. \end{cases} \quad (1.17)$$

This domain on the phase diagram, where smooth menisci exist, forms the square shown in Fig. 3*a*).

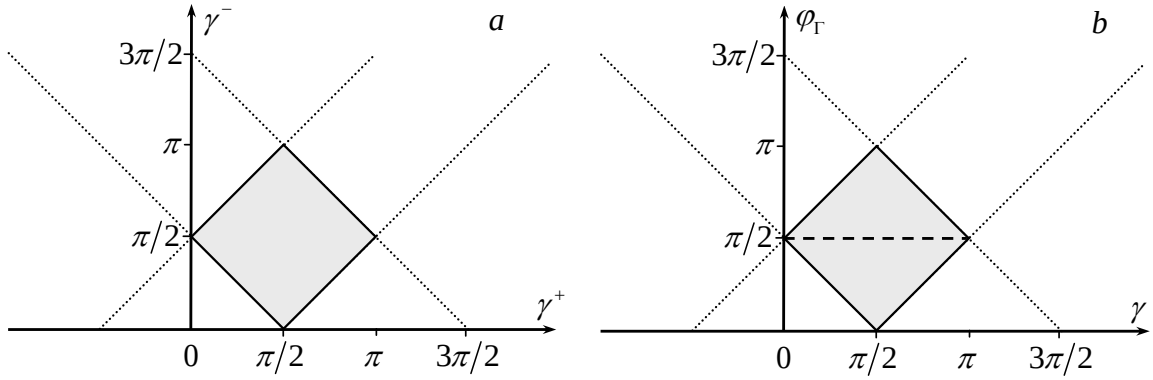

Figure 3. (*a*) square of the admissible angles γ^{+}, γ^{-} where the interiors, $\varphi_{\Gamma} = \pi/4$, and exteriors, $\varphi_{\Gamma} = 3\pi/4$, of the square corner are able to form smooth menisci; (*b*) The wetting phase diagram for a particular case of the chemically homogeneous V-shaped edge, $\gamma^{+} = \gamma^{-} = \gamma$. The internal smooth menisci correspond to the triangle below the dashed line and the external smooth menisci correspond to the triangle above the dashed line.

Remarkably, the conditions for formation of smooth menisci inside and outside the square corner appear the same! Therefore, this particular square geometry does not distinguish the wetting conditions when the meniscus is about to jump up the groove inside the corner due to the suction capillary pressure, or fall down the edge outside the corner due to the squeezing capillary pressure.

A chemically heterogeneous V-shaped edge with two surfaces having completely different wetting properties deserves a special attention.

V-shaped Janus edge, $\gamma^{+} = 0$, $\gamma^{-} = \pi$. The first eq (1.10) give $A_1 = 0$, and the second equation can be rewritten as $\sqrt{1 + A_2^{-2}} = \cos\varphi_{\Gamma}$. Since the left hand side of this equation is always greater than 1, one cannot find any φ_{Γ} to satisfy this equation. Therefore, one cannot form a smooth meniscus on any V-shaped Janus edge.

However, if one relaxes the smoothness condition by allowing the following solutions to occur

$$r \ll 1: \quad h(r, \varphi) = F_0(\varphi), \qquad where \qquad F_0(\varphi) \neq Const\,, \quad (1.18)$$

A quasi-smooth meniscus can be obtained. This solution for a quasi-smooth meniscus has to satisfy the following equation $(F_0'/|F_0'|)'=0$, which has the solution $(F_0'/|F_0'|)=const$. Due to definition, the ratio $F_0'/|F_0'|$ is the unit tangent vector to the curve $F_0(\varphi)$, hence if the function $F_0(\varphi)$ is not a constant, one always has $(F_0'/|F_0'|)=\pm 1$. This condition does not contradict the boundary condition at the edge surface $\Gamma=\Gamma^+\cup\Gamma^-$ where

$$\left.\frac{F_0'(\varphi)}{|F_0'(\varphi)|}\right|_{\varphi=\pm\varphi_\Gamma}=\pm\cos\gamma^{\pm}\equiv 1. \tag{1.19}$$

Taking, for example $F_0(\varphi)=B_1+B_2\varphi$, with a positive constant B_2 and arbitrary constant B_1, we obtain a helicoid [12]

$$h(r,\varphi)=B_1+B_2\varphi,\qquad B_2>0, \tag{1.20}$$

Any helicoid satisfies eq. (1.3) everywhere within the plane (r,φ), but it cannot satisfy the Young-Laplace eq. (1.4) on the full faces of V-shaped edge [12]. It only satisfies the boundary conditions in the vicinity of point O where $r\ll 1$. Even though, the helicoid singular solution can be a good candidate to describe a transition region from one face to the other.

Consider another cross-section $\gamma^+=\gamma^-=\gamma$ of the 3D wetting phase diagram in the space of parameters $(\gamma^+,\gamma^-,\varphi_\Gamma)$.

Chemically homogeneous V-shaped edge, $\gamma^+=\gamma^-=\gamma\in[0,\pi]$; $\varphi_\Gamma\in(0,\pi]$. In this case, meniscus is symmetric with respect to the axis $\varphi=0$. As follows from eqs. (1.10), the constant $A_2=0$ is always equal to zero. The constant A_1 is determined from equation

$$A_1=-\frac{\cos\gamma}{\sqrt{\sin^2\varphi_\Gamma-\cos^2\gamma}} \tag{1.21}$$

This constant is the real valued one if and only if the following inequality holds true

$$\sin^2\varphi_\Gamma-\cos^2\gamma>0. \tag{1.22}$$

Thus, a smooth meniscus (1.13) exists only within a certain range of the corner angles satisfying condition (1.22). The latter can be rewritten in the form $\sin^2\varphi_\Gamma-\cos^2\gamma=-\cos(\gamma+\varphi_\Gamma)\cos(\gamma-\varphi_\Gamma)>0$ implying that the following two constraints on the contact angle have to be satisfied

$$\frac{3\pi}{2}>\gamma+\varphi_\Gamma>\frac{\pi}{2}, \tag{1.23}$$

$$-\frac{\pi}{2}<\gamma-\varphi_\Gamma<\frac{\pi}{2}. \tag{1.24}$$

These conditions lead to the diagram shown in Fig. 3*b*). It relates the contact angle γ with the angle φ_Γ. Another interpretation of condition (1.22) can be inferred by rewriting it as $\sin^2\varphi_\Gamma > \sin^2(\pi/2-\gamma)$. The right hand side of this inequality reaches the maximum when the difference $\pi/2-\gamma$ becomes equal to $\pm\pi/2$. Therefore, the inequality holds true for:

а) Wetting case, $\gamma<\pi/2$: when the corner angle φ_Γ is nearer to $\pi/2$, relative to the proximity of angle γ to 0.

б) Non-wetting case: $\gamma>\pi/2$: when the corner angle φ_Γ is nearer to $\pi/2$, relative to the proximity of angle γ to π.

It is worth to remind the famous Concus-Finn condition for formation of a nonsingular meniscus in a V-shaped groove, $\varphi_\Gamma > |\gamma-\pi/2|$ [9]. This condition is included in eqs. (1.23), (1.24). Since eq. (1.22) is applicable for both internal and external menisci, the derived conditions are valid for both types of menisci.

Thus, in the vicinity of point O the asymptotic solution of the boundary value problem (1.3), (1.5) for the chemically homogeneous edge takes on the form

$$r \ll 1: \qquad h(r,\varphi) \approx F^o + A_1 r\cos\varphi \qquad \Leftrightarrow \qquad h(x,y) \approx F^o + A_1 x\,. \tag{1.25}$$

This implies that in the first approximation, the surface of the smooth meniscus is always planar. This planar surface Σ is shown schematically in Fig. 3*b*). It meets the fiber at slope A_1. One can imagine the meniscus surface as a sheet of paper with the removed V-piece (like a pie piece) and then inserted into the wedge at some angle $\pi-\alpha$. The angle α is related to the slope as $A_1=\tan\alpha$; in the wetting case it is negative, in the non-wetting case it is positive.

It appears that the Concus-Finn condition is much weaker than the condition based on the derived solution. In Fig. 3*b*) the dashed line separates the external menisci from the internal ones: the upper triangle corresponds to the external menisci while the lower triangle corresponds to the internal menisci.

In the wetting case, $\gamma<\pi/2$, smooth solution (1.25) for the internal menisci does not exist in the very narrow corners. As shown by Concus and Finn [9], the narrow corners are filled with the long narrow liquid fingers running along the corners. The explanation is that the narrow fingers generate a strong *negative* capillary pressure sucking up the meniscus. At very high negative capillary pressure, the finger is almost vertical, hence the h-function cannot describe the meniscus any more.

It is interesting to observe that our condition of existence of the smooth solution suggests that the ribbon-like ($\varphi_\Gamma=\pi$) wettable fibers do not have a smooth contact line either. The Concus-Finn hypothesis about a finger-like meniscus collected at the vertex fails in this case. Indeed, contrary to the internal meniscus, any film covering the exterior of the corner edge would generate a strong *positive* capillary pressure which would tend to squeeze the liquid out of this. The

mechanism is exactly the same: a negative capillary pressure in the grooves pulls the liquid into the groove, while a positive capillary pressure at the edge pushes the liquid out from the film that connects two opposite sides of the meniscus. The arrows in Figure 2 indicate a jump of the end point of the contact line along the film edge. The contact line is still continuous, but it is described by a step-like function, i.e. its derivative is discontinuous. Hence, it is difficult to believe that the breakup of the solution continuity through its derivatives is the only possible scenario of the singular behavior of wetting menisci.

In the non-wetting case, $\gamma > \pi/2$, the narrow corners repel the internal menisci. Flipping the Concus-Finn argument toward the air, one would expect to have some bubbles forming steep finger-like menisci trapped at the corners. Again, the behavior of meniscus at the edges of non-wettable ribbon ($\varphi_\Gamma = \pi$) is much more complicated and deserves a special attention. In general, the full experimental and theoretical analysis of possible singularities would help design different microfluidic devices with prescribed wetting properties.

With these 2D phase diagrams in hands, we are ready to move on and discus the 3D phase diagrams of wetting transitions. The 2D phase diagrams will help us to double check the validity of the 3D construction.

Chemically inhomogeneous V-shaped edge, $\varphi_\Gamma \in (0,\pi]$, $\gamma^+ \in [0,\pi]$, $\gamma^- \in [0,\pi]$. In the general 3D case, it is convenient to consider eq. (1.12) as the definition of a parabola with respect to the variable $\xi = \cos 2\varphi_\Gamma$

$$\Phi(\xi) = (1 - \cos^2\gamma^+ - \cos^2\gamma^-) - 2\cos\gamma^+\cos\gamma^-\xi - \xi^2 . \tag{1.26}$$

In the plane (ξ, Φ), the branches of parabola are pointing down, therefore, a smooth meniscus occurs only within the following interval

$$\xi_1 < \xi < \xi_2 , \tag{1.27}$$

where ξ_1 is the smallest real valued root and ξ_2 is the largest real valued root of the quadratic equation $\Phi(\xi) = 0$. The discriminant D of this quadratic equation is always positive,

$$D = 4\sin^2\gamma^+\sin^2\gamma^- > 0 . \tag{1.28}$$

Hence the quadratic equation has two real valued roots

$$\xi_{1,2} = -\cos\gamma^+\cos\gamma^- \pm \sin\gamma^+\sin\gamma^- = -\cos\left(\gamma^+ \pm \gamma^-\right). \tag{1.29}$$

Substituting $\xi = \cos 2\varphi_\Gamma$, and expressing the largest and smallest roots through the contact angles, we obtain from condition (1.27) the following criterion for the existence of a smooth solution (1.13) in the 3D phase space ($\gamma^+, \gamma^-, \varphi_\Gamma$):

$$\min\left[-\cos\left(\gamma^{+}-\gamma^{-}\right),-\cos\left(\gamma^{+}+\gamma^{-}\right)\right]<\ \cos 2\varphi_{\Gamma}\ <\max\left[-\cos\left(\gamma^{+}-\gamma^{-}\right),-\cos\left(\gamma^{+}+\gamma^{-}\right)\right].\quad(1.30)$$

In order to find the domain in 3D space defined by inequality (1.30), we first need to determine the boundaries of this domain. This boundary is described by equations

$$\cos\left(\gamma^{+}+\gamma^{-}\right)=-\cos\left(2\varphi_{\Gamma}\right),\tag{1.31}$$

$$\cos\left(\gamma^{+}-\gamma^{-}\right)=-\cos\left(2\varphi_{\Gamma}\right).\tag{1.32}$$

Taking into account the constraints on the angles, $\gamma^{+}\in[0,\pi]$, $\gamma^{-}\in[0,\pi]$, $\varphi_{\Gamma}\in(0,\pi]$, we see that the angles involved in eqs. (1.31), (1.32) change within the following intervals

$$\left(\gamma^{+}+\gamma^{-}\right)\in[0,2\pi],\quad\left(\gamma^{+}-\gamma^{-}\right)\in[-\pi,\pi],\quad 2\varphi_{\Gamma}\in(0,2\pi].\tag{1.33}$$

Solving eq. (1.31) for the angles defined by eq. (1.33), we obtain four plane boundaries

$$\begin{aligned}&\varphi_{\Gamma}\in(0,\pi/2]:\qquad\gamma^{+}+\gamma^{-}=\pi-2\varphi_{\Gamma},\quad\gamma^{+}+\gamma^{-}=\pi+2\varphi_{\Gamma};\\&\varphi_{\Gamma}\in[\pi/2,\pi]:\qquad\gamma^{+}+\gamma^{-}=2\varphi_{\Gamma}-\pi,\quad\gamma^{+}+\gamma^{-}=3\pi-2\varphi_{\Gamma}.\end{aligned}\tag{1.34}$$

With the same constraints (1.33), eq. (1.32) generates two plane boundaries

$$\varphi_{\Gamma}\in(0,\pi]:\qquad\gamma^{+}-\gamma^{-}=\pi-2\varphi_{\Gamma},\quad\gamma^{+}-\gamma^{-}=2\varphi_{\Gamma}-\pi\,.\tag{1.35}$$

In order to make a geometrical construction of the 3D phase diagram in space $(\gamma^{+},\gamma^{-},\varphi_{\Gamma})$ we introduce the following points $O_1=(\pi,0,0)$, $O_2=(0,\pi,0)$, $O_3=(0,0,\pi/2)$, $O_4=(\pi,\pi,\pi/2)$, $O_5=(\pi,0,\pi)$, $O_6=(0,\pi,\pi)$, separated by the distances $|O_1O_2|=|O_3O_4|=|O_5O_6|=\pi\sqrt{2}$, $|O_1O_3|=|O_1O_4|=|O_2O_3|=|O_2O_4|=\pi\sqrt{5}/2$, and $|O_5O_3|=|O_5O_4|=|O_6O_3|=|O_6O_4|=\pi\sqrt{5}/2$. Using these points, one can draw planes (1.31), (1.32) as

$$\begin{aligned}&\gamma^{+}+\gamma^{-}=\pi-2\varphi_{\Gamma}\ &\rightarrow\ &\ plane\ O_1O_2O_3;\\&\gamma^{+}+\gamma^{-}=\pi+2\varphi_{\Gamma}\ &\rightarrow\ &\ plane\ O_1O_2O_4;\\&\gamma^{+}+\gamma^{-}=2\varphi_{\Gamma}-\pi\ &\rightarrow\ &\ plane\ O_3O_5O_6;\\&\gamma^{+}+\gamma^{-}=3\pi-2\varphi_{\Gamma}\ &\rightarrow\ &\ plane\ O_4O_5O_6;\\&\gamma^{+}-\gamma^{-}=\pi-2\varphi_{\Gamma}\ &\rightarrow\ &\ plane\ O_1O_3O_4O_6;\\&\gamma^{+}-\gamma^{-}=2\varphi_{\Gamma}-\pi\ &\rightarrow\ &\ plane\ O_2O_3O_4O_5.\end{aligned}\tag{1.36}$$

Using these boundaries, we have to assign the space domains where inequalities (1.30) hold true. With the examples that we discussed earlier, the 3D domain satisfying all conditions can be identified straightforwardly by considering different 2D cross-sections and matching them with the

solved examples. It appears that the interiors of tetrahedrons O_1,O_2,O_3,O_4 and O_3,O_4,O_5,O_6 satisfy all the required constrains, Fig. 4. These tetrahedrons have the common edge O_3,O_4, and they are mirror symmetric with respect to the plane $\varphi_\Gamma = \pi/2$.

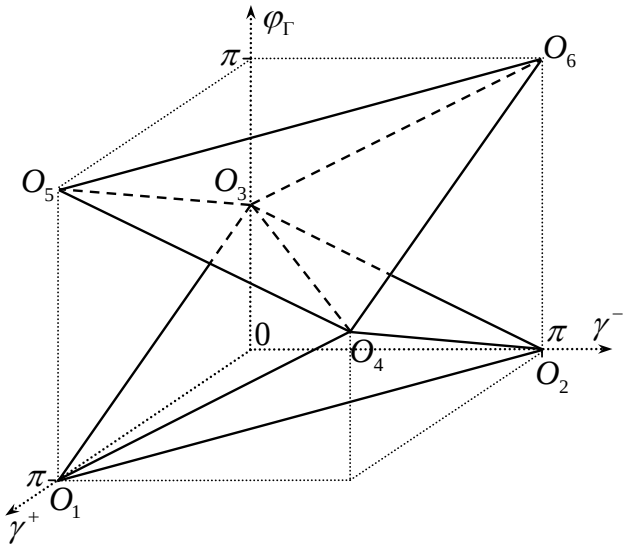

Figure 4. The interiors of tetrahedrons O_1,O_2,O_3,O_4 and O_3,O_4,O_5,O_6 correspond to the smooth menisci.

In summary, this Letter addressed the problem of classification of menisci with respect to their behavior at the V-type edges. While different numerical methods have been developed in recent years, the criteria for formation of singularities of the contact lines and menisci formed on the complex shaped slender fibers are still unknown and are actively discussed in the literature. In this Letter, we discovered new criteria for smoothness of the menisci formed at the V-type edges with chemically different faces. In the case of an arbitrary opening angle φ_Γ of the V-shaped edge, the wetting phase diagram has been drawn in the 3D space of parameters $(\gamma^+,\gamma^-,\varphi_\Gamma)$. We illustrated the obtained criteria using chemically inhomogeneous plates, blades, square corners, and Janus V-shaped edges. In the case of a homogeneous V-shaped edge, these criteria relate the contact angle and the V-angle and specify the window defined by eq. (1.23), (1.24) when a smooth meniscus occurs. An analysis proposed here significantly enlarges the famous Concus-Finn condition for the existence of a smooth meniscus.

K. G. K. was supported by the National Science Foundation through the Grant PoLS 1305338. M. M. A. was supported by the Russian Foundation for Basic Research, projects Nos. 12-01-00996 and 13-01-00368.

References

[1] J. Jurin, "An Account of Some Experiments Shown before the Royal Society; With an Enquiry into the Cause of the Ascent and Suspension of Water in Capillary Tubes. ," *Philosophical Transactions of the Royal Society,* vol. 30, pp. 739-747, January 1, 1717 1717.

[2] D. A. White and J. A. Tallmadge, "Static menisci on outside of cylinders," *Journal of Fluid Mechanics,* vol. 23, pp. 325-&, 1965 1965.

[3] B. Miller and R. A. Young, "Methodology for studying wettability of filaments," *Textile Research Journal,* vol. 45, pp. 359-365, 1975.

[4] B. Miller, "The wetting of fibers," in *Surface characteristics of fibers and textiles*. vol. 2, M. J. Schick, Ed., ed New York: Marcel Dekker, 1977, pp. 417-445.

[5] B. Miller, *et al.*, "Wetting force measurements on single fibers," *Colloids and Surfaces,* vol. 6, pp. 49-61, 1983.

[6] A. W. Adamson and A. P. Gast, *Physical chemistry of surfaces*. New York: Wiley, 1997.

[7] A. Tuteja, *et al.*, "Robust omniphobic surfaces," *PNAS,* vol. 105, pp. 18200-18205, Nov 2008.

[8] W. Choi, *et al.*, "A modified Cassie–Baxter relationship to explain contact angle hysteresis and anisotropy on non-wetting textured surfaces," *Journal of Colloid and Interface Science,* vol. 339, pp. 208-216, 2009.

[9] P. Concus and R. Finn, "On behavior of a capillary surface in a wedge," *Proceedings of the National Academy of Sciences of the United States of America,* vol. 63, pp. 292-&, 1969.

[10] P. S. Laplace, *Mecanique Celeste*, 5 ed. vol. IV. New York: Chelsea Publishing Company, 1966.

[11] T. Young, "An Essay on the Cohesion of Fluids," *Philosophical Transactions of the Royal Society of London,* vol. 95, pp. 65-87, January 1, 1805 1805.

[12] J. Oprea, *Differential geometry and its applications*, 2nd ed. Washington DC: The Mathematical Association of America, 2007.

[13] J. B. Keller, "Surface tension force on a partly submerged body," *Physics of Fluids,* vol. 10, pp. 3009-3010, 1998.

[14] M. M. Alimov and K. G. Kornev "Meniscus on a shaped fibre: singularities and hodograph formulation," *Proc. R. Soc. A* vol. 470, p. 20140113, 2014.